Infrared Multiphoton Dissociation Spectroscopy of Cationized Serine: Effects of Alkali-Metal Cation Size on Gas-Phase Conformation

P. B. Armentrout,*,† M. T. Rodgers,*,‡ J. Oomens,§ and J. D. Steill§

Department of Chemistry, University of Utah, Salt Lake City, Utah 84112, Department of Chemistry, Wayne State University, Detroit, Michigan 48202, and FOM Institute for Plasma Physics "Rijnhuizen", Edisonbaan 14, 3439 MN Nieuwegein, The Netherlands

Received: November 14, 2007; In Final Form: February 5, 2008

The gas-phase structures of alkali-metal cation complexes of serine (Ser) are examined using infrared multiple photon dissociation (IRMPD) spectroscopy utilizing light generated by a free electron laser, in conjunction with ab initio calculations. Spectra of Li^+(Ser) and Na^+(Ser) are similar and relatively simple, whereas Cs^+(Ser) includes distinctive new IR bands, and K^+(Ser) and Rb^+(Ser) exhibit intermediate behavior. Measured IRMPD spectra are compared to spectra calculated at a B3LYP/6-311+G(d,p) level to identify the structures present in the experimental studies. On the basis of these experiments and calculations, the only conformations accessed for the complexes to the smaller alkali-metal cations, Li^+ and Na^+, are charge-solvated structures involving tridentate coordination to the amine and carbonyl groups of the amino acid backbone and to the hydroxyl group of the side chain, M1[N,CO,OH]. For the cesiated complex, a band corresponding to a zwitterionic structure, ZW[CO_2^-], is clearly visible. K^+(Ser) and Rb^+(Ser) exhibit evidence of the charge-solvated analogue of the zwitterions, M3[COOH], in which the metal cation binds to the carboxylic acid group. Calculations indicate that the relative stability of the M3[COOH] structure is very strongly dependent on the size of the metal cation, consistent with the range of conformations observed experimentally.

Introduction

Recently, the pairwise interactions of serine (Ser) and threonine (Thr) with the alkali-metal cations, Li^+, Na^+, and K^+, were studied using guided ion beam mass spectrometry.[1] Quantitative bond dissociation energies were determined and found to be consistent with theoretical values predicted for the ground state conformations, charge-solvated structures involving tridentate binding to the amine and carbonyl groups of the amino acid backbone combined with interaction with the side-chain hydroxyl group, M1[N,CO,OH] (see below for a definition of the nomenclature used). A quantitative assessment of such pairwise interactions is potentially useful as they play an important role in many biological systems. For instance, sodium cations drive the transport of free serine and threonine and their peptide forms into an asaccharolytic, gram-negative bacterium called porphyromonas gingivalis.[2]

In the case of the M^+(Ser) complexes where $M^+ = Li^+$, Na^+, and K^+, the M1[N,CO,OH] ground state conformation is calculated to lie well below (>8 kJ/mol) any other conformations, such that quantitative bond energy measurements are sufficient to determine the identity of the complexes formed experimentally.[1] However, calculations also show that the energy gaps between the ground state and excited conformations narrow as the size of the metal cation increases. This is consistent with observations made in our laboratory regarding the ground state conformation of metalated glycine, Na^+(Gly) vs K^+(Gly),[3,4] as well as other metal cationized amino acids.[5−11] For Na^+(Gly), the predicted ground state conformer is M1[N,CO] where the metal cation binds to the backbone amine and carbonyl groups, whereas K^+(Gly) prefers to bind to the carboxylic acid group, M3[COOH]. Our analysis of the trends in the interactions of these metal cations with the functional components of glycine indicate that this change in structure occurs largely because the binding energy to the amino group is relatively weak for the larger potassium cation (or relatively strong for the smaller sodium cation) compared to the other functional sites on glycine. The conformation of Na^+(Gly) has been documented using IR spectra,[12] although no similar results are yet available for K^+(Gly). Given these trends, it is of interest to explore the conformations of metal cationized serine for the heavier alkali-metal cations, Rb^+ and Cs^+. As threshold collision-induced dissociation measurements are not sufficiently precise to enable small differences in conformational energy to be distinguished, the use of infrared multiphoton dissociation (IRMPD) is used to examine whether the conformations of experimentally generated complexes change as a function of metal cation size. Identification of the conformations present is achieved by comparison to IR spectra derived from ab initio calculations of the low-lying structures of these complexes with optimized structures and vibrational frequencies determined at the B3LYP/6-311+G(d,p) level of theory. In a companion study,[39] similar measurements and calculations are performed for the analogous M^+(Thr) complexes and the results are compared to the present findings for M^+(Ser).

Experimental and Computational Section

Mass Spectrometry and Photodissociation. A 4.7 T Fourier-transform ion cyclotron resonance (FTICR) mass spectrometer was used in these experiments and has been described in detail elsewhere.[13−15] Tunable radiation for the photodissociation experiments is generated by the free electron laser for infrared experiments (FELIX).[16] For the present experiments, spectra

† University of Utah.
‡ Wayne State University.
§ FOM Institute for Plasma Physics "Rijnhuizen".

10.1021/jp710885a CCC: $40.75
Published on Web 02/21/2008

were recorded over the wavelength range 19.4 μm (520 cm^{-1}) to 5.5 μm (1820 cm^{-1}). Pulse energies were around 50 mJ per macropulse of 5 μs duration, although they fell off to about 20 mJ toward the blue edge of the scan range. The fwhm bandwidth of the laser was typically 0.5% of the central wavelength. Serine was obtained from Aldrich. Cationized amino acids were formed by electrospray ionization using a Micromass Z-Spray source and a solution of 3.0 mM amino acid and 0.5−1.0 mM alkali-metal chloride in 70%:30% MeOH/H_2O solutions. Solution flow rates ranged from 15 to 30 μL/min and the electrospray needle was generally held at a voltage of ~3.2 kV. Ions were accumulated in a hexapole trap for about 4 s prior to being injected into the ICR cell via an rf octopole ion guide. Electrostatic switching of the dc bias of the octopole allows ions to be captured in the ICR cell without the use of a gas pulse, thus avoiding collisional heating of the ions.[14] All complexes except Li^+(Ser) were irradiated for 3 s, corresponding to interaction with 15 macropulses, whereas the Li^+(Ser) complexes were irradiated for 4 s and thus interacted with 20 macropulses.

Computational Details. In previous work,[1] Ye and Armentrout examined all likely conformers of serine and its complexes with Li^+, Na^+, and K^+ using a simulated annealing procedure that combines annealing cycles and ab initio calculations.[3] Briefly, the AMBER program and the AMBER force field based on molecular mechanics[17] were used to search for possible stable structures in each system's conformational space. All possible structures identified in this way were further optimized using NWChem[18] at the HF/3-21G level.[19,20] Unique structures for each system within 50 kJ/mol of the lowest energy structure (~30 for each complex) were further optimized using Gaussian 03[21] at the B3LYP/6-31G* level[22,23] with the "loose" keyword (maximum step size of 0.01 au and an rms force of 0.0017 au) to facilitate convergence. Because serine has 2S chirality, this property is constrained throughout the annealing simulations. The 10−15 lowest energy structures obtained from this procedure were then chosen for higher level geometry optimizations and frequency calculations using density functional theory (DFT) at the B3LYP/6-311+G(d,p) level.[24,25] This level of theory has been shown to provide reasonably accurate structural descriptions of comparable metal−ligand systems.[3,4] Single point energy calculations were carried out for the 6−15 most stable structures at the B3LYP, B3P86, and MP2(full) levels using the 6-311+G(2d,2p) basis set.[24] Zero-point vibrational energy (ZPE) corrections were determined using vibrational frequencies calculated at the B3LYP/6-311+G(d,p) level scaled by a factor of 0.9804.[26]

For the Rb^+ and Cs^+ complexes studied here, all conformations considered previously for K^+(Ser) were used as starting points for geometry and vibrational frequency calculations optimized at the B3LYP/HW*/6-311+G(d,p) level where HW* indicates that Rb and Cs were described using the effective core potentials (ECPs) and valence basis sets of Hay and Wadt[27] with a single d polarization function (exponents of 0.24 and 0.19, respectively) included.[28] Relative energies are determined using single point energies at the B3LYP, B3P86, and MP2(full) levels using the HW*/6-311+G(2d,2p) basis set. In addition, similar HW* calculations were performed for the K^+(Ser) complexes to assess the accuracy of the Hay−Wadt ECP/ valence basis sets (exponent of 0.48 for the d polarization function on K).

Vibrational frequencies and intensities were calculated using the harmonic oscillator approximation and analytical derivatives of the energy-minimized Hessian calculated at the B3LYP/HW*/6-311+G(d,p) level of theory. Frequencies were scaled by 0.9804, to eliminate known systematic errors.[26] For comparison to experiment, calculated vibrational frequencies are broadened using a 20 cm^{-1} fwhm Gaussian line shape.

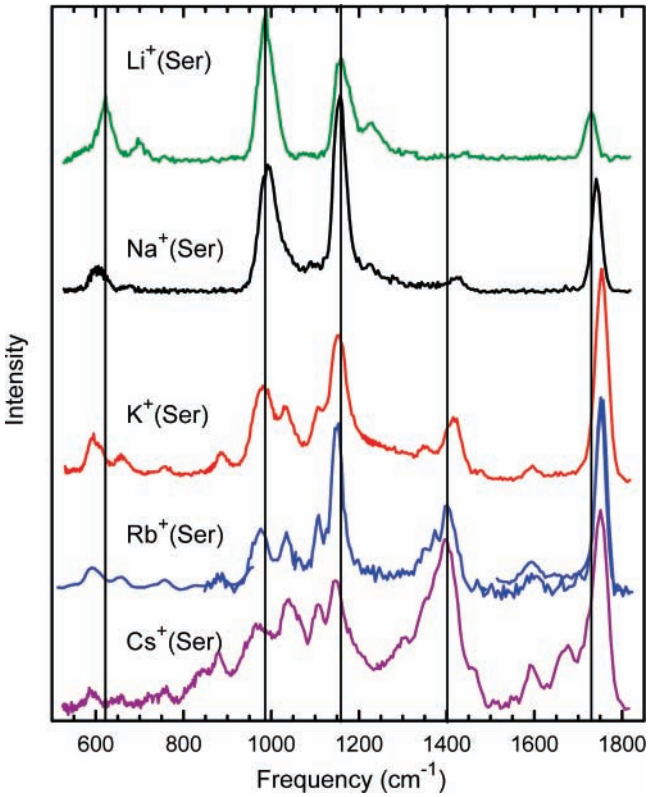

Figure 1. Infrared multiphoton dissociation action spectra of M^+(Ser) complexes where $M^+ = Li^+$, Na^+, K^+, Rb^+, and Cs^+.

Results and Discussion

IRMPD Action Spectroscopy. Photodissociation of M^+(Ser), where $M^+ = Na^+$, K^+, Rb^+, and Cs^+, result in the loss of the intact ligand to form the atomic metal cation, consistent with collision-induced dissociation (CID) results for the sodiated and potassiated complexes.[1] IRMPD action spectra are taken from the relative intensity of the M^+ product cation as a function of laser wavelength, as shown in Figure 1. No corrections for laser power were applied but would primarily enhance the intensities observed at the highest laser frequencies.

For Li^+(Ser), where the metal cation binding affinity is the largest, the CID spectra exhibit several low-energy channels corresponding to loss of H_2O, H_2O + CO, CH_2O, CO_2, and H_2O + CO_2 from the complex as well as formation of $Li^+(H_2O)$.[1] The first three of these product channels are observed upon photodissociation with H_2O loss having the highest intensity (about twice that of the other two channels). This is in rough agreement with the CID results that show that these three product ions have the largest cross sections among the six observed channels, with H_2O loss being about twice as large as the other two channels, which in turn are about twice as large as the Li^+(Ser−CO_2) and Li^+(Ser−H_2O−CO_2) channels. Formation of $Li^+(H_2O)$ is a higher energy channel, explaining its absence in the IRMPD results. The sum of these three channels is shown as the IRMPD action spectrum in Figure 1. No significant effect of the laser frequency on the branching ratio of the H_2O and H_2CO fragmentation pathways was observed over the range of wavelengths investigated, whereas the H_2O + CO channel exhibits mild variations compared to the H_2O

TABLE 1: Relative Energies at 0 K and Free Energies at 298 K (kJ/mol) of Low-Lying Conformers of M^+(Ser)[a]

name	structure	B3LYP	B3P86	MP2(full)
Li^+(Ser)	**M1[N,CO,OH]-*cis*-OH**	**0.0 (0.0)**	**0.0 (0.0)**	**0.0 (0.0)**
	M1[N,CO]	23.8 (21.0)	23.1 (20.3)	29.6 (26.8)
	M8[CO,OH]	24.7 (22.1)	24.1 (21.5)	35.8 (33.2)
	M1[N,CO,OH]-*trans*-OH	26.0 (25.0)	25.7 (24.7)	27.1 (26.1)
	M5[N,OH,OH]	29.7 (28.4)	30.8 (29.5)	25.4 (24.1)
	ZW[CO_2^-]	33.7 (30.9)	29.6 (26.8)	36.6 (33.8)
	TS(M3-ZW)	56.7 (54.1)	47.7 (45.4)	61.6 (59.2)
	M3[COOH]	61.1 (51.1)	55.7 (45.7)	66.0 (56.0)
Na^+(Ser)	**M1[N,CO,OH]-*cis*-OH**	**0.0 (0.0)**	**0.0 (0.0)**	**0.0 (0.0), 0.0**[b]
	ZW[CO_2^-]	20.5 (18.2)	16.0 (13.6)	23.6 (21.3), 24.7[b]
	M1[N,CO]	21.6 (18.6)	20.9 (17.9)	26.0 (23.0), 44.4[b]
	M8[CO,OH]	24.2 (21.8)	22.3 (20.0)	32.7 (30.3), 50.6[b]
	M1[N,CO,OH]-*trans*-OH	26.3 (26.1)	25.7 (25.5)	26.9 (26.7)
	M5[N,OH,OH]	27.8 (27.4)	29.2 (28.8)	24.8 (24.4), 25.1[b]
	TS(M3-ZW)	31.4 (29.5)	22.0 (20.1)	34.9 (33.0)
	M3[COOH]	31.8 (28.1)	26.7 (23.0)	35.0 (31.3)
K^+(Ser)	**M1[N,CO,OH]-*cis*-OH**	**0.0 (0.0)**	**0.0 (0.0)**	**0.0 (0.0)**
		0.0 (0.0)	***0.0 (0.0)***	***0.0 (0.0)***
	M3[COOH]	10.1 (6.6)	8.9 (5.4)	17.9 (14.4)
		11.2 (7.4)	*7.7 (4.0)*	*17.9 (14.1)*
	ZW[CO_2^-]	11.0 (9.3)	8.2 (6.5)	18.5 (16.9)
		13.1 (11.5)	*8.8 (7.2)*	*21.6 (20.0)*
	TS(M3-ZW)	14.3 (12.7)	7.7 (6.1)	22.2 (20.6)
		16.2 (14.5)	*7.4 (5.7)*	*23.8 (22.0)*
	M8[CO,OH]	14.5 (11.8)	15.6 (12.9)	25.9 (23.1)
		15.9 (13.2)	*14.6 (11.9)*	*26.7 (24.0)*
	M1[N,CO]	15.3 (12.8)	15.9 (13.3)	21.6 (19.0)
		16.4 (14.0)	*16.2 (13.7)*	*23.6 (21.2)*
	M1[N,CO,OH]-*trans*-OH	24.1 (22.5)	25.0 (23.4)	26.2 (24.6)
		25.2 (24.9)	*24.9 (24.6)*	*24.8 (24.4)*
	M5[N,OH,OH]	25.0 (24.4)	27.5 (26.9)	23.7 (23.2)
		25.9 (25.3)	*26.9 (26.4)*	*22.2 (21.7)*
Rb^+(Ser)	**M1[N,CO,OH]-*cis*-OH**	***0.0*** *(1.0)*	*1.0 (4.1)*	***0.0 (0.0)***
	M3[COOH]	*2.1* ***(0.0)***	***0.0 (0.0)***	*11.0 (7.8)*
	TS(M3-ZW)	*10.5 (10.5)*	*2.9 (5.0)*	*19.5 (18.5)*
	ZW[CO_2^-]	*10.6 (10.5)*	*7.4 (9.3)*	*20.4 (19.2)*
	M8[CO,OH]	*12.1 (10.0)*	*12.0 (12.0)*	*23.0 (19.9)*
	M1[N,CO]	*13.0 (11.5)*	*14.0 (14.7)*	*20.2 (17.7)*
	M1[N,CO,OH]-*trans*-OH	*24.7 (25.2)*	*25.5 (28.1)*	*25.7 (25.2)*
	M5[N,OH,OH]	*24.8 (25.1)*	*26.6 (29.1)*	*22.0 (21.3)*
Cs^+(Ser)	**M3[COOH]**	***0.0 (0.0)***	***0.0 (0.0)***	*5.3 (2.1)*
	M1[N,CO,OH]-*cis*-OH	*4.0 (7.2)*	*6.8 (10.0)*	***0.0 (0.0)***
	TS (M3-ZW)	*11.2 (13.7)*	*5.6 (8.1)*	*16.3 (15.6)*
	M8[CO,OH]	*13.3 (13.5)*	*15.1 (15.3)*	*19.5 (16.6)*
	ZW[CO_2^-]	*13.5 (15.8)*	*11.8 (14.2)*	*19.1 (18.2)*
	M1[N,CO]	*14.0 (14.7)*	*17.0 (17.8)*	*16.7 (14.3)*
	M5[N,OH,OH]	*27.6 (30.1)*	*31.0 (33.5)*	*21.7 (21.0)*
	M1[N,CO,OH]-*trans*-OH	*28.1 (30.8)*	*30.6 (33.2)*	*25.0 (24.5)*

[a] Free energies in parentheses. All values calculated at the level of theory indicated using the 6-311+G(2d,2p) basis set with structures and zero point energies calculated at the B3LYP/6-311+G(d,p) level of theory. Values in italics use the HW* basis set on the metal. [b] Reference 34.

loss channel. In this secondary product channel, the bands at 620, 700, and 1230 cm^{-1} have about half the intensity of the primary H_2O loss channel, those at 980 and 1720 cm^{-1} are about one-third the intensity, and that at 1160 cm^{-1} about 80% of the intensity. In addition, there is a slight blue shift in the 1720 cm^{-1} band for H_2O loss compared with those for the other two channels. This behavior is consistent with H_2O loss being the lowest energy dissociation channel, as previously found in the CID results.[1] In IRMPD spectroscopy, a slight red shift in absorption bands is often observed for higher energy dissociation channels and is caused by the increased influence of vibrational anharmonicity.[29,30]

Comparison of the spectra in Figure 1 shows that the features observed in the Li^+(Ser) spectrum are retained for all of the metal cation complexes, but that new spectral features begin to appear for K^+(Ser) and become very obvious for Cs^+(Ser). The band at 1720 cm^{-1} shifts to the blue as the metal cation becomes heavier, those at 620 and 700 cm^{-1} shift to the red, and the bands in the middle (980 and 1170 cm^{-1}) exhibit minor shifts to the red for the heavier metal cations.

Theoretical Results. A detailed discussion of the structures of serine and its metal cation complexes with Li^+, Na^+, and K^+ can be found elsewhere.[1] As described above, complexes with Rb^+ and Cs^+ were calculated here at the B3LYP/HW*/6-311+G(d,p) level starting with the structures of all low-lying potassiated complexes located previously, a total of seven conformations. The nomenclature used to identify these different structural isomers is taken from that established previously for Na^+Gly.[3,31,32] Briefly, neutral serine is designated as N*x* where *x* indicates one of three main types of structural isomers with different modes of intramolecular hydrogen bonding. This is followed by a notation that indicates the relative position (either trans = t or gauche = g) of the −OH group to the carbonyl carbon and its relative position to the amino nitrogen. Conformations of M^+(Ser) are identified as M*y* (where *y* refers to a specific structure as first designated by Jensen for glycine

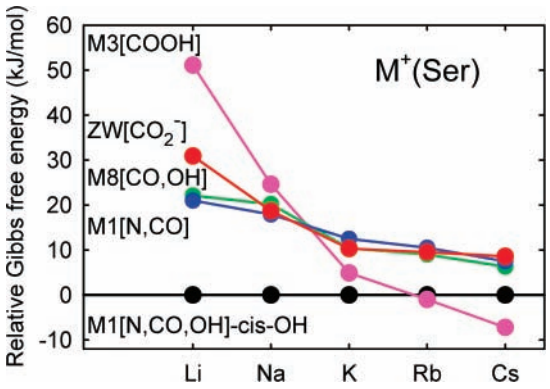

Figure 2. Gibbs free energies (kJ/mol) calculated at the B3LYP level of theory (Table 1) of five conformations of M^+(Ser) complexes as a function of the alkali-metal cation identity relative to the energy of the M1[N,CO,OH]-*cis*-OH conformer.

complexes[33]) augmented by a notation in brackets that describes the metal binding sites for each isomer. The zwitterionic conformer is designated as ZW[CO_2^-].

Single point energies including zero point energy (ZPE) corrections calculated at three different levels of theory, relative to the lowest energy isomer, are given in Table 1 for M^+(Ser). The MP2/6-31G(d)//HF/6-31+G(d) results for Na^+(Ser) calculated by Hoyau et al.[34] are also included in Table 1 and agree well with our MP2(full) values determined at a higher level of theory. Given this agreement, our values are used in the following discussion for consistency. Table 1 also lists the relative free energies at 298 K of these conformers. These values may be more relevant in the determination of the experimental distribution. Values for K^+(Ser) calculated using the HW* ECP rather than the all electron basis set give very similar relative energies, within 3 kJ/mol for all enthalpies and free energies of all conformations, Table 1. Therefore, the all electron values will be used throughout the remaining discussion. The overall trends in the relative free energies are shown in Figure 2 for the B3LYP results and are very similar to those of the relative enthalpies at 0 K. The main difference arises because tridentate binding of the M1[N,CO,OH] and M5[N,OH,OH] conformers leads to a smaller entropic contributions for these conformers such that they become relatively less stable compared to the bidentate binding conformers, by about 2−4 kJ/mol.

All three levels of theory find that the N2-g,g structure is the ground state conformer of serine.[1] Five other low-lying conformations have also been described and are found to lie within 10 kJ/mol at all levels of theory.[1] The N2 type of structure is characterized by a COH···N hydrogen bond (1.92 Å) with an additional C_βO···HN hydrogen bond (2.49 Å), and a third, long-distance (2.82 Å) C_βOH···O=C hydrogen bond.

The low-lying structures found for all M^+(Ser) complexes are illustrated by those for Cs^+(Ser) shown in Figure 3. Several important geometric parameters for the M^+(Ser) complexes are provided in Table 2. For most of the alkali-metal cations, the ground state structure is the tridentate charge-solvated M1[N,CO,OH]-*cis*-OH conformer, where *cis*-OH indicates that the carboxylic hydrogen is cis relative to the carbonyl oxygen. We note that the M^+−OC, M^+−N, and M^+−OH distances increase from 1.97 to 3.14 Å, 2.09 to 3.38 Å, and 1.98 to 3.25 Å, respectively, as the size of the metal cation increases from Li^+ to Cs^+. These changes directly reflect the increase in the ionic radius of the metal cation (0.70 Å for Li^+, 0.98 Å for Na^+, 1.33 Å for K^+, 1.49 Å for Rb^+, and 1.69 Å for Cs^+)[35] coupled with the resultant decreasing charge density, which weakens the electrostatic interaction with serine. The ∠M^+OC

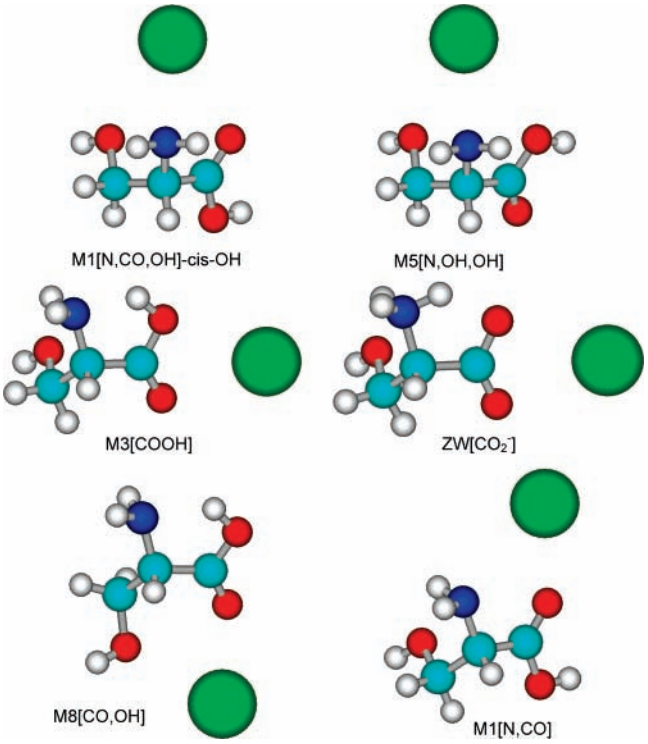

Figure 3. Structures of the Cs^+(Ser) complexes calculated at the B3LYP/HW*/6-311+G(d,p) level of theory.

bond angle increases with the size of the cation, consistent with elongations of the M^+−OC and M^+−N distances. Notably the ∠M^+OCC_α and ∠NC_αCO dihedral angles increase and decrease, respectively, from Li^+ to Cs^+ for the same reason. For example, tighter binding to the higher charge density Li^+ moves the three ligating groups closer to the metal cation, such that the ∠M^+OCC_α dihedral angle for Li^+(Ser) is closer to planar than for the heavier metals, Table 2.

For Cs^+(Ser) and Rb^+(Ser), the DFT calculations indicate that the M3[COOH] conformer is the ground state (or nearly the ground state), Table 1. The M3[COOH] conformation is closely related to the zwitterionic structure, ZW[CO_2^-], with the main difference being the location of the proton bridging the COH and amine groups, Figure 3. The zwitterionic structure lies 26−30 and 10−12 kJ/mol lower than the M3 structure for Li^+(Ser) and Na^+(Ser), respectively, whereas ZW lies above M3 by 7−10 and 12−14 kJ/mol for Rb^+(Ser) and Cs^+(Ser), respectively. For K^+(Ser), the two structures are nearly isoenergetic, lying within 1 kJ/mol of one another at all levels of theory.

Transition states (TSs) between ZW[CO_2^-] and M3[COOH] were located using the synchronous transit-guided quasi-newton (STQN) method of Schlegel and co-workers[36] or relaxed potential energy surface scans at the B3LYP/HW*/6-311+G(d,p) level. Single point energies were calculated at the three levels listed above using the 6-311+G(2d,2p) or HW*/6-311+G(2d,2p) basis sets. Energies for these TSs with ZPE corrections included were found to be 18−25, 6−12, and −2 to +4 kJ/mol higher in energy than the ZW[CO_2^-] conformer for M^+ = Li^+, Na^+, and K^+, respectively, whereas those for M^+ = Rb^+ and Cs^+ are 0−5 and 2−6 kJ/mol *lower*, respectively. When compared to the energies of the M3[COOH] isomer, the TSs are 4−8 and 0−5 kJ/mol lower for M^+ = Li^+ and Na^+, respectively, and −1 to +4, 2−9, and 5−11 kJ/mol higher for M^+ = K^+, Rb^+, and Cs^+, respectively. Thus, once ZPEs are included, the M3[COOH] complexes of Li^+(Ser) and Na^+(Ser) collapse to the lower energy zwitterion with no barrier

TABLE 2: Geometric Parameters of M^+(Ser) Structures[a]

	$r(M^+-O)$ (Å)[b]					$r(M^+-N)$ (Å)					$r(M^+-O)$ (Å)				
conformer	Li	Na	K	Rb	Cs	Li	Na	K	Rb	Cs	Li	Na	K	Rb	Cs
M1[N,CO,OH]-*cis*-OH	1.968	2.318	2.667 *2.687*	*2.919*	*3.144*	2.091	2.452	2.857 *2.876*	*3.134*	*3.382*	1.975	2.342	2.740 *2.760*	*3.011*	*3.252*
M3[COOH]	1.911	2.285	2.636 *2.662*	*2.907*	*3.119*						2.104	2.428	2.849 *2.876*	*3.103*	*3.387*
ZW[CO_2^-]	1.930	2.283	2.627 *2.660*	*2.893*	*3.103*						1.960	2.325	2.681 *2.700*	*2.942*	*3.175*
M1[N,CO,OH]-*trans*-OH	1.939	2.289	2.626 *2.645*	*2.868*	*3.086*	2.110	2.480	2.902 *2.922*	*3.197*	*3.454*	1.980	2.344	2.756 *2.769*	*3.025*	*3.273*
M1[N,CO]	1.857	2.224	2.569 *2.591*	*2.822*	*3.037*	2.033	2.428	2.872 *2.894*	*3.177*	*3.445*					
M5[N,OH,OH]	2.018	2.378	2.804 *2.814*	*3.088*	*3.393*	2.051	2.415	2.810 *2.829*	*3.083*	*3.323*	1.941	2.305	2.686 *2.702*	*2.948*	*3.174*
M8[CO,OH]	1.810	2.170	2.513 *2.534*	*2.771*	*2.982*						1.901	2.306	2.740 *2.756*	*3.022*	*3.293*

	$\angle M^+OC$ (deg)					$\angle M^+OCC_\alpha$ (deg)					$\angle NC_\alpha CO$ (deg)				
conformer	Li	Na	K	Rb	Cs	Li	Na	K	Rb	Cs	Li	Na	K	Rb	Cs
M1[N,CO,OH]-*cis*-OH	103.8	108.1	113.0 *113.2*	*114.6*	*116.3*	11.6	18.7	26.6 *26.6*	*32.9*	*36.9*	32.8	28.0	22.2 *22.4*	*17.9*	*15.4*
M3[COOH]	93.6	97.0	102.4 *102.7*	*104.0*	*107.4*	178.0	177.8	177.2 *177.4*	*176.9*	*177.5*	175.8	175.6	175.5 *175.4*	*175.4*	*174.8*
ZW[CO_2^-]	84.0	88.8	92.7 *92.6*	*94.6*	*96.6*	178.1	178.0	178.0 *177.5*	*178.2*	*178.6*	168.8	169.4	170.0 *170.1*	*170.6*	*170.8*
M1[N,CO,OH]-*trans*-OH	106.3	111.1	116.9 *117.2*	*119.2*	*120.7*	10.0	17.1	25.0 *24.9*	*31.1*	*36.9*	34.7	30.0	24.8 *25.0*	*21.3*	*17.7*
M1[N,CO]	113.6	119.8	127.2 *127.5*	*130.6*	*133.7*	1.0	2.0	5.9 *5.6*	*10.1*	*12.4*	7.9	8.1	6.6 *6.6*	*5.5*	*4.2*
M5[N,OH,OH]	106.4[c]	109.9[c]	112.1[c] *112.4*[c]	*112.1*[c]	*110.4*[c]	14.6[d]	23.4[d]	33.0[d] *33.1*[d]	*40.3*[d]	*46.8*[d]	150.4	155.7	162.4 *162.3*	*167.3*	*172.4*
M8[CO,OH]	129.6	138.2	146.3 *146.5*	*149.6*	*152.9*	6.4	1.7	0.7 *1.8*	*4.8*	*6.5*	168.0	165.7	164.4 *163.9*	*162.3*	*161.0*

[a] Values calculated at the B3LYP/6-311+G(d,p) or B3LYP/HW*/6-311+G(d,p) (italics) levels of theory. [b] The carbonyl oxygen in all cases except M5[N,OH,OH] where it is the carboxylic oxygen. [c] $\angle M^+O(H)C_\alpha$ (deg). [d] $\angle M^+O(H)CC_\alpha$ (deg).

to the proton transfer, whereas for Rb^+(Ser) and Cs^+(Ser), the zwitterion collapses to the lower energy M3[COOH] conformer. For K^+(Ser), the two conformations are essentially isoenergetic such that there is a small barrier at the B3LYP and MP2 levels of theory (3−4 kJ/mol above ZW[CO_2^-]), but no barrier at the B3P86 level, Table 1. (To test whether these results were sensitive to the level of theory chosen for the geometry optimizations, calculations for the relative energies of ZW[CO_2^-], M3[COOH], and the TS for K^+(Ser) were also performed with geometries optimized at the B3P86/HW*/6-311+G(d,p) and B3LYP/HW*/6-311+G(2d,2p) levels of theory followed by single point calculations at the same three levels of theory used elsewhere. Overall, the same trends are found with average energy differences from the values obtained using the B3LYP/HW*/6-311+G(d,p) geometries of -0.5 ± 0.5 and 0.4 ± 0.6 kJ/mol, respectively. The qualitative conclusions drawn above remain.)

Several other alternative conformations for the M^+(Ser) complexes were also identified, but their relative energies change little with metal cation and all remain at least 10 kJ/mol higher than the ground state structure, Table 1 and Figure 2. These alternative conformations include M1[N,CO,OH]-*trans*-OH, which is almost identical to M1[N,CO,OH]-*cis*-OH except that the carboxylic hydrogen is trans to the carbonyl oxygen, such that no intramolecular hydrogen bond is formed between them. Breaking this intramolecular hydrogen bond costs nearly the same amount of energy for all five metal cations, 22−27 kJ/mol. If the metal cation interaction with the backbone groups is maintained but the side-chain interaction is lost, the bidentate conformer, M1[N,CO], is obtained. This conformer lies 23−30, 21−26, 15−22, 13−20, and 14−17 kJ/mol above M1[N,CO,OH]-*cis*-OH for Li^+-Cs^+, respectively, Table 1. The changes in the relative energies from Li^+ to Cs^+ reflect the stronger binding to the smaller cations. These bidentate structures have shorter M^+-OC bond distances than the M1[N,CO,OH]-*cis*-OH conformer by about 0.10 Å for all five metals, which can be explained by less steric constraints in the bidentate configuration. In contrast, the relative M^+-N distances change appreciably as a function of the metal cation, decreasing by about 0.06 and 0.02 for Li^+ and Na^+, respectively, but increasing by 0.02, 0.04, and 0.06 Å for K^+, Rb^+, and Cs^+, respectively. These changes occur despite the relaxed steric constraints and emphasize that the metal cation interaction with the amino group weakens as the metal cation size increases more appreciably than the interactions with other functional groups.

In the M8[CO,OH] structure, M^+ interacts in a bidentate fashion with the carbonyl and side-chain hydroxyl oxygen atoms, Figure 3. The energy of this conformer relative to the M1[N,CO,OH]-*cis*-OH conformer drops by about 16 kJ/mol in going from Li^+(Ser) to Cs^+(Ser). In another tridentate isomer, M5[N,OH,OH], M^+ binds to the hydroxyl oxygen of the carboxylic group instead of the carbonyl oxygen, Figure 3. This less favorable interaction[3,4,37] leads to excitation energies of 21−31 kJ/mol above the M1[N,CO,OH]-*cis*-OH conformer, with only a mild dependence on metal cation identity.

Overall, the relative energetics of the various conformations as a function of metal cation identity are shown in Figure 2. The relative energies for most conformations do not change appreciably, with the obvious exception of the M3[COOH] conformer, which drops appreciably as the metal cation gets larger and more diffuse. As noted in the introduction, M3[COOH] is the calculated ground state conformation of

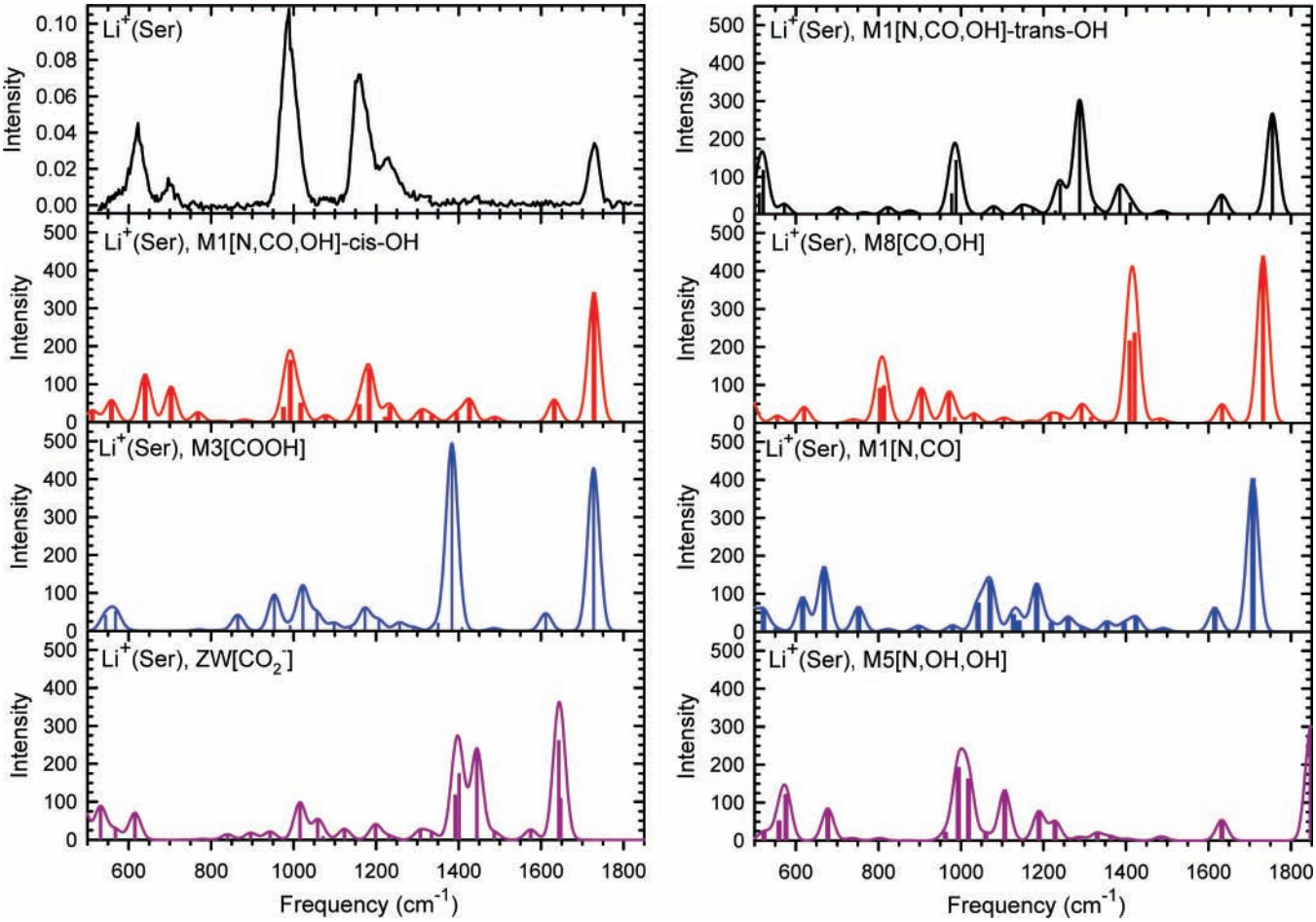

Figure 4. Comparison of the experimental IRMPD action spectrum for Li^+(Ser) with IR spectra for seven conformations predicted at the B3LYP/6-311+G(d,p) level of theory.

K^+(Gly),[4] compared to the M1[N,CO] structure found for Li^+(Gly) and Na^+(Gly).[3,12,37] This difference in the preferred binding geometry has been attributed to relatively stronger interactions with the amino group as the metal cation gets smaller (higher charge density). For Ser, because the metal cation interacts with the side-chain hydroxyl group as well as with the amino and carbonyl groups of the backbone, the M1[N,CO,OH] conformation is stabilized relative to the M3[COOH] conformation, such that the change in ground state conformation toward M3[COOH] is shifted from a transition point between Na^+(Gly) and K^+(Gly) to the heavier metals for M^+(Ser).

Comparison of Experimental and Theoretical IR Spectra: Li^+(Ser) and Na^+(Ser). Figure 4 shows the experimental IRMPD action spectrum along with calculated IR spectra for the seven low-energy conformers found for the Li^+(Ser) complex. In making these comparisons, one should keep in mind that the calculated IR intensities often do not correspond well with the action spectrum because the latter is a multiphoton process, whereas the theoretical IR intensities are based on single photon absorption. Given that proviso, it is clear that the bands predicted for the M1[N,CO,OH]-*cis*-OH conformer correspond well with the observed spectrum. All major bands are present with comparable theoretical and experimental frequencies. The largest differences are found for the bands between 600 and 700 cm^{-1}, where there is a blue shift in the predicted band positions. Some minor bands predicted are not observed experimentally, notably at 1420 and 1630 cm^{-1}, which is probably because the multiphoton dissociation probability is small for these weak bands. However, several minor bands predicted theoretically do have corresponding small features in the experimental spectrum, e.g., at 760, 1070, and 1320 cm^{-1}.

The highest frequency band observed, 1730 cm^{-1}, corresponds to the carbonyl stretch, which explains its large predicted intensity. Interaction with the lithium cation results in a red shift of this band compared to that for free Ser, calculated as 1791 cm^{-1} for N2-gg. Thus, this band is found at a similar frequency for most of the Li^+(Ser) conformations, with the exceptions being M5[N,OH,OH] and ZW[CO_2^-]. In the former system, the metal cation does not bind to the carbonyl group, in contrast to all other conformations, such that the CO stretch has a frequency blue-shifted from that of bare Ser. For the zwitterion, the CO stretch is red-shifted even more because its functionality has changed from a carboxylic acid to a carboxylate moiety.

The experimentally observed bands at 980 and 1150 cm^{-1} with a shoulder at 1230 cm^{-1}, are probably the most diagnostic bands for the M1[N,CO,OH]-*cis*-OH structure. The relative intensities of these three bands as well as their positions are nicely predicted by the IR spectrum for this conformer. No other conformations are predicted to have this sequence of frequencies. Indeed weak bands at 1080 and 1320 cm^{-1} also seem consistent with the experimental spectrum in this region. At lower frequencies, the experimental spectrum exhibits bands at 620 and 700 cm^{-1}, which corresponds reasonably well with the predicted spectrum for M1[N,CO,OH]-*cis*-OH except that the former band is blue-shifted compared with experiment. This frequency corresponds to the wagging motion of the carboxylic acid hydrogen atom, such that a blue shift suggests that the calculations overestimate the strength of the hydrogen bond

between this hydrogen atom and the carbonyl group. Below ~600 cm^{-1}, the laser power is insufficient to adequately address whether the relative intensities are meaningful. Although other conformations also have bands in this region of the spectrum, the combination of these two strong bands are best reproduced by the M1[N,CO,OH]-*cis*-OH conformer. Again, the very minor band at 760 cm^{-1} might also agree with the predicted spectrum for this conformation.

A reviewer suggests that the spectrum for the M1[N,CO] structure, the second lowest energy conformer, is also in rough agreement with the observed IRMPD spectrum. However, this conformer has its carbonyl stretch shifted to 1708 cm^{-1} (about 20 cm^{-1} lower than experiment and the 1728 cm^{-1} prediction for the M1[N,CO,OH]-*cis*-OH conformer) and the band corresponding to the 980 cm^{-1} experimental band is at 1042 and 1071 cm^{-1} (compared to 992 cm^{-1} for the M1[N,CO,OH]-*cis*-OH conformer). Although such comparisons cannot completely rule out the presence of any conformer, we conclude that the experimental spectrum is well represented by that calculated for the ground state M1[N,CO,OH]-*cis*-OH conformer.

As shown in Figure 1, the IRMPD action spectra for Li^+-(Ser) and Na^+(Ser) are very similar, exhibiting all of the same major spectral features. Comparison of experimental and theoretical spectra for Na^+(Ser) can be found in the Supporting Information, Figure S1. Subtle differences include a blue-shift in the band at ~1730 cm^{-1} (to ~1750 cm^{-1}); a red-shift in the band at ~620 cm^{-1} (to ~600 cm^{-1}); and a new band at 1430 cm^{-1} (although some intensity in this region may also exist for the Li^+(Ser) spectrum). The calculated spectrum for the M1[N,CO,OH]-*cis*-OH conformer of Na^+(Ser) shows a close correspondence with the experimental spectrum, comparable to that obtained for Li^+(Ser). The calculated spectra correctly predict a blue shift in the 1730 cm^{-1} band of 15 cm^{-1} and a red shift in the 620 cm^{-1} band of 15 cm^{-1}. The band at 1430 cm^{-1} is also consistent with the predicted spectrum for this conformer, and was also present in the predicted spectrum for Li^+(Ser). It might also be noted that there is an increase in intensity between the two bands at 980 and 1160 cm^{-1} of the Na^+(Ser) spectrum, which matches a band predicted for the M1[N,CO,OH]-*cis*-OH conformer of Na^+(Ser) at 1094 cm^{-1}. The comparable band in the Li^+(Ser) spectrum lies closer to the major peak at slightly lower energy, and hence is not observed as readily. We again conclude that the experimental spectrum is well represented by that calculated for the ground state M1[N,CO,OH]-*cis*-OH conformer.

Comparison of Experimental and Theoretical IR Spectra: K^+(Ser) and Rb^+(Ser). Figure 5 shows the experimental IRMPD action spectrum of K^+(Ser) compared with theoretical predictions for the three lowest energy conformations calculated (consistent for all three levels of theory used, Table 1). (It can be noted that vibrational frequencies calculated using the all electron vs the HW* basis sets on K yield results that differ by an average of less than 0.03%. Hence, the use of the HW* basis sets for the Rb and Cs systems should yield equivalent results to the all electron basis sets used for the smaller cations.) Compared with the experimental spectrum for Na^+(Ser), the K^+(Ser) spectrum retains all the same bands, but new features are now evident (or possibly better resolved). The appearance of these new bands could be evidence for new conformers or could be the result of better sensitivity associated with more facile dissociation of this more weakly bound system. The K^+−Ser bond energy has been measured as 145 ± 7 kJ/mol as compared with those for Na^+−Ser of 200 ± 8 kJ/mol[1] or the loss of H_2O from Li^+(Ser) of about 199 ± 14 kJ/mol.[40] The

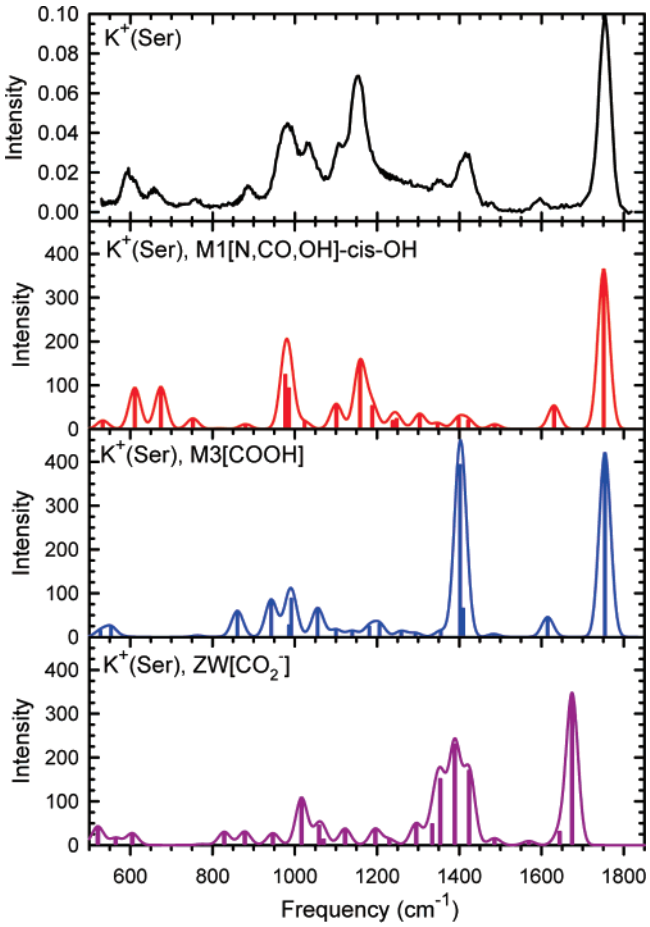

Figure 5. Comparison of the experimental IRMPD action spectrum for K^+(Ser) with IR spectra for three low-lying conformations predicted at the B3LYP/6-311+G(d,p) level of theory.

spectrum for Rb^+(Ser) is similar to that for K^+(Ser), Figure 1, with the same number of new bands compared to the Na^+(Ser) spectrum. Comparison of experimental and theoretical spectra for Rb^+(Ser) can be found in the Supporting Information, Figure S3. The calculated bond energy for the Rb^+(Ser) system is still weaker, 103−120 kJ/mol, which should again lead to greater sensitivity.

New bands in the spectra for K^+(Ser) and Rb^+(Ser) occur at ~760, 880, 1030, 1110, 1350, and 1590 cm^{-1}. In addition, the band at 1420 cm^{-1} grows in intensity compared to that for Na^+(Ser) and there is a general increase in intensity in the region between this band and the band at 1150 cm^{-1}. For many of these spectral features, there is a corresponding band in the predicted spectrum of the M1[N,CO,OH]-*cis*-OH conformer, Figure 5. The worst discrepancies are probably the weak predicted intensities of the bands at 1030, 1350, and 1420 cm^{-1} and the blue shift in the predicted band at 1630 cm^{-1} (vs 1590 cm^{-1} observed). Therefore, we consider whether the M3[COOH] conformer might be contributing to the observed spectra for K^+(Ser) and Rb^+(Ser). As the calculations indicate that this conformation is low-lying for K^+(Ser) and perhaps the ground state for Rb^+(Ser), this is certainly reasonable. The dominant feature in the predicted spectrum for M3[COOH] overlaps directly with the CO stretch feature in the M1[N,CO,OH]-*cis*-OH spectrum at 1750 cm^{-1}. The other obvious band in the M3[COOH] spectrum is the large feature at 1400 cm^{-1}, which could explain the increased intensity in the band at 1420 cm^{-1}. Other bands in the M3[COOH] spectrum in the vicinity of 1000 cm^{-1} overlap the comparable bands in the M1[N,CO,OH]-

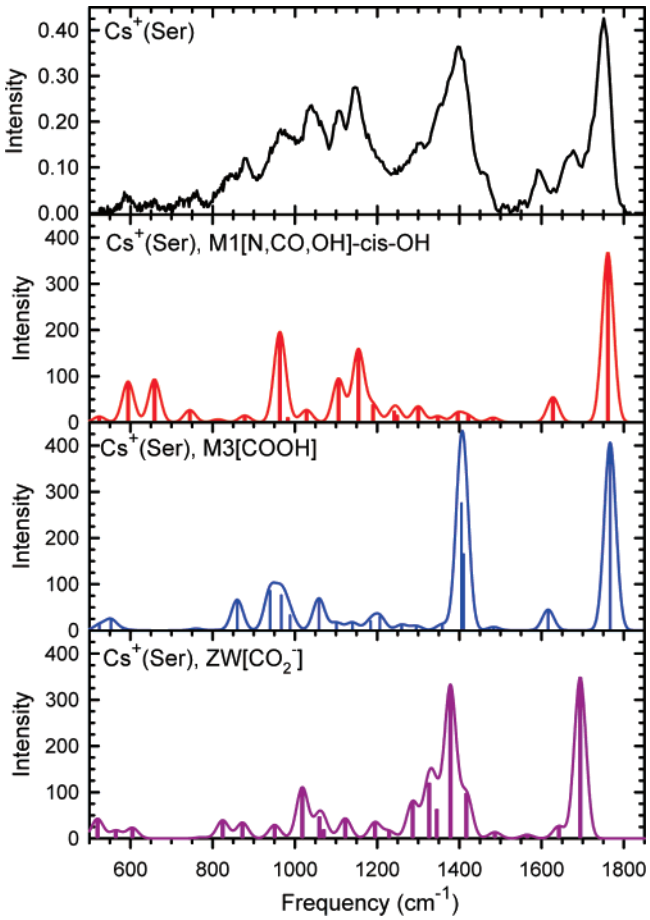

Figure 6. Comparison of the experimental IRMPD action spectrum for Cs^+(Ser) with IR spectra for three low-lying conformations predicted at the B3LYP/HW*/6-311+G(d,p) level of theory.

cis-OH spectrum, although it is possible that the most intense of these can explain the new band observed at 1030 cm^{-1}.

Neither the M3[COOH] nor the M1[N,CO,OH]-*cis*-OH spectra calculated for K^+(Ser) and Rb^+(Ser) predict the bands observed at 1590 cm^{-1} very accurately, but all other conformers except ZW predict a similar frequency (see Figure 4 for the analogous situation of Li^+(Ser)). This band corresponds almost exclusively to a NH_2 bending motion in both conformations and is largely unperturbed from the 1620 cm^{-1} band predicted for neutral serine (N2-gg). It is possible that this band could be a combined contribution of the comparable bands in the M3[COOH] and M1[N,CO,OH]-*cis*-OH spectra, helping to explain the observed shift. It also seems likely that the harmonic approximation of the calculated potential gives somewhat inaccurate vibrational frequencies for this particular mode, as has been observed for NH_2 bending modes in other systems.[29,38]

Comparison of Experimental and Theoretical IR Spectra: Cs^+(Ser). The IRMPD action spectrum of Cs^+(Ser) is clearly the most complicated of all five metal cation systems, Figure 1. The details of this spectrum were confirmed over the range 1000−1800 cm^{-1} by acquisition at reduced power (by 3 dB). Comparison of the experimental spectrum with those calculated for three key conformers is shown in Figure 6. The spectrum is fairly similar to that of Rb^+(Ser), but with new bands at ~840 and 1680 cm^{-1}, along with a much broader band peaked at 1400 cm^{-1}, and with a possible new peak at 1310 cm^{-1}. The peak at 1680 cm^{-1} is most diagnostic and clearly corresponds to the zwitterionic conformer, ZW[CO_2^-], which has a predicted band at 1694 cm^{-1}. In addition, the much broader peak at 1400 cm^{-1} is consistent with the presence of this conformation, as are the other minor changes observed. Because of the large intensity of the peak at 1400 cm^{-1}, it seems likely that the M3[COOH] conformation is also present. The retention of the major features observed in the spectra for the smaller metal cations also indicates that the M1[N,CO,OH]-*cis*-OH continues to be present as well. The appearance of multiple conformers is consistent with the relative enthalpies and free energies calculated for this system, Table 1.

It may seem contradictory that evidence for the ZW conformer is found even though the calculations find no energetic barrier between the ZW and M3 conformers for Cs^+(Ser) once zero point energies are included. In thinking about this observation, it can be realized that there must still be a phase space limit (lower density of states) between the conformers because of the barrier along the electronic surface. This plausibly allows the system to exist in the ZW conformation for sufficient time to allow IRMPD to occur. A different way of thinking of this same dynamic issue is to appreciate that the hydrogen stretching motion that converts between the ZW and M3 conformers is high frequency, calculated to be 3144 cm^{-1} (ZPE = 18.8 kJ/mol) for M3 of Cs^+(Ser) and 2820 cm^{-1} (ZPE = 16.9 kJ/mol) for ZW of Cs^+(Ser). Thus, the former ZPE lies above or close to the height of the barrier, 19.4, 13.8, and 19.2 kJ/mol above the M3 conformer without ZPE correction at the B3LYP, B3P86, and MP2(full) levels of theory, respectively. Viewed from the ZW potential well, the barrier heights without ZPE correction are 7.5, 3.5, and 6.9 kJ/mol, well below the 16.9 kJ/mol ZPE of the reaction coordinate for M3-ZW interconversion. Clearly, the potential surface along this coordinate is no longer harmonic, such that the calculated frequencies are unlikely to be accurate. However, it seems plausible that the ground state wavefunction for this vibration includes components in both the M3 and ZW potential energy wells, thereby allowing IR absorption in the orthogonal degrees of freedom probed in these experiments for both conformers.

It is also interesting that the presence of the ZW conformer seems relatively obvious in the spectrum of Cs^+(Ser), but not in the spectra of K^+(Ser) and Rb^+(Ser). In contrast, the calculated relative energies of Figure 2 suggest that the ZW conformer is actually less stable for Cs^+(Ser) than the other two metal cations relative to the ground state. However, examination of Table 1 shows that the DFT levels of theory favor the M3[COOH] and ZW[CO_2^-] conformations compared to the M1[N,CO,OH]-*cis*-OH conformer, whereas the MP2(full) level of theory is the opposite. At the latter level of theory, it can be seen that the relative free energy of the ZW conformer at 298 K increases from 18 kJ/mol for Cs^+(Ser) to 19 and 20 kJ/mol for Rb^+(Ser) and K^+(Ser), respectively. In addition, the relative free energy of the M3 conformer increases from 2 to 8 to 14 kJ/mol, respectively. Taken overall, it seems plausible that once the M3 conformer is thermally populated (as it certainly is for Cs^+(Ser) with lower populations for the lighter metal cations), the phenomenon suggested in the previous paragraph makes the ZW conformer accessible for Cs^+(Ser), but less so for the lighter metal cations. This analysis also suggests that the MP2(full) level of theory provides more accurate relative energies of these various conformations.

Overview. We can now provide a more global comparison of the main features in all five spectra. A detailed list of the theoretically predicted frequencies and IR intensities for the three main conformers of M^+(Ser) are provided as Tables S1−S3 in the Supporting Information. The predicted frequencies for the CO stretch of the M1[N,CO,OH]-*cis*-OH conformer change from 1728 cm^{-1} for Li^+(Ser), to 1743 cm^{-1} (Na^+(Ser)), to

1751 cm^{-1} (K^+(Ser)), to 1758 cm^{-1} (Rb^+(Ser)), and finally to 1761 cm^{-1} for Cs^+(Ser), in good agreement with the blue shift observed in the spectra, Figure 1. However, this shift is not conformation specific as the shifts are comparable for the M3[COOH] conformer: 1755, 1765, and 1767 cm^{-1} for K^+(Ser), Rb^+(Ser), and Cs^+(Ser), respectively. These shifts are clearly the result of a decreased perturbation on the CO stretch with decreased metal cation binding strength. Likewise the low-energy band in the Li^+(Ser) spectrum at 620 cm^{-1} (an out-of-plane bending motion of the carboxylic hydrogen atom) red shifts to about 580 cm^{-1} for Cs^+(Ser). The predicted spectral features for the M1[N,CO,OH]-*cis*-OH conformer also shift by a comparable amount, from 640 cm^{-1} for Li^+(Ser), to 626 cm^{-1} for Na^+(Ser), 611 cm^{-1} for K^+(Ser), 600 cm^{-1} for Rb^+(Ser), and 594 cm^{-1} for Cs^+(Ser).

As noted above, bands at ~980 and 1160 cm^{-1} in the Li^+(Ser) spectrum have a modest red shift of about 20 cm^{-1}, Figure 1. (These bands have motions that involve a side-chain C−O stretch combined with an NH_2 bend and concerted COH bends of both hydroxyl groups, respectively.) The predicted bands in this region for the M1[N,CO,OH]-*cis*-OH conformer shift from 992 and 1183 cm^{-1} for Li^+(Ser), to 992 and 1162 cm^{-1} for Na^+(Ser), 977/986 and 1159 cm^{-1} for K^+(Ser), 971 and 1156 cm^{-1} for Rb^+(Ser), and 963 and 1154 cm^{-1} for Cs^+(Ser). Again the trends are in remarkably good agreement with the observed spectra, suggesting that the assignment of these features to the M1 conformation is appropriate.

For the M3[COOH] conformer of K^+(Ser), the most diagnostic band appears at 1402 cm^{-1} (where the motion is an in-plane bend of the carboxylic hydrogen), with a predicted intensity comparable to that of the band for the CO stretch at 1755 cm^{-1}. This conformer is predicted to exhibit less intense bands at 860, 943, 991, and 1056 cm^{-1} (with motions approximated by an NH_2 bend, NH_2 bend, out-of-plane bend of the carboxylic hydrogen, and $C_\alpha-C_\beta$ stretch, respectively). The major band shifts little for Rb^+(Ser), 1403 cm^{-1}, and Cs^+(Ser), 1405 cm^{-1}, which agrees roughly with the observations in Figure 1. The minor bands at 860, 943, and 1056 cm^{-1} shift very little for Rb^+(Ser), 859, 940, and 1056 cm^{-1}, and for Cs^+(Ser), 860, 940, and 1058 cm^{-1}, whereas the minor band at 991 cm^{-1} for K^+(Ser) shifts to 974 and 967 cm^{-1} for Rb^+(Ser) and Cs^+(Ser), respectively. These bands fall under similar bands in the M1[N,CO,OH]-*cis*-OH spectrum, which shift similarly with metal cation identity. The bands at 860 and 1056 cm^{-1}, which do not appear in the Li^+(Ser) and Na^+(Ser) spectra, are more diagnostic. These bands are observed to shift very little for K^+(Ser), Rb^+(Ser), and Cs^+(Ser), in agreement with the predictions for the M3[COOH] conformation.

Conclusions

The IRMPD action spectra of the alkali-metal cationized amino acid serine in the region 600−1800 cm^{-1} have been obtained for five alkali-metal cations, $M^+ = Li^+$, Na^+, K^+, Rb^+, and Cs^+. Comparison of these experimental spectra with IR spectra calculated at the B3LYP/6-311+G(d,p) and B3LYP/HW*/6-311+G(d,p) levels of theory allow the conformations likely to be present in the experiment to be identified. Present results suggest that only the tridentate M1[N,CO,OH]-*cis*-OH conformation is present for the Li^+(Ser) and Na^+(Ser) complexes, in agreement with the predicted ground states of these complexes. For the K^+(Ser) and Rb^+(Ser) complexes, the presence of the M3[COOH] conformer along with the M1[N,CO,OH]-*cis*-OH conformer is indicated. For the Cs^+(Ser) complex, these same two conformers are joined by the zwitterionic conformer, ZW[CO_2^-]. This progression in relative stabilities parallels that elucidated for metalated tryptophan complexes, although no evidence for the zwitterion is found in this system.[11] For the M^+(Ser) systems, theory finds that the M3[COOH] conformer becomes the ground state for the heavier metal systems, consistent with its observation in their spectra. The large change in the relative stabilities of the M1[N,CO,OH]-*cis*-OH and M3[COOH] conformers can be rationalized on the basis of the strength of the M^+−amine interaction as a function of the metal cation.[3,4] The smaller metal cations bind relatively more strongly to the amine, favoring the M1 structure, whereas the heavier more diffuse metal cations prefer binding to the carboxylic acid site.

Acknowledgment. This work is part of the research program of FOM, which is financially supported by the Nederlandse Organisatie voor Wetenschappeklijk Onderzoek (NWO). Additional financial support was provided by the National Science Foundation, Grants PIRE-0730072, CHE-0451477 and CHE-0748790 (P.B.A.), and CHE-0528262 (M.T.R.). The skillful assistance of the FELIX staff is gratefully acknowledged.

Supporting Information Available: Four figures showing a comparison between the experimental IRMPD spectrum and theoretically predicted IR spectra of seven low-lying conformations of Na^+(Ser), K^+(Ser), Rb^+(Ser), and Cs^+(Ser). Three tables (S1−S3) providing the vibrational frequencies and IR intensities for the M1[N,CO,OH]-*cis*-OH, M3[COOH], and ZW[CO_2^-] conformations for M^+(Ser) calculated at the B3LYP/6-311+G(d,p) ($M^+ = Li^+$, Na^+, and K^+) or B3LYP/HW*/6-311+G(d,p) ($M^+ = Rb^+$ and Cs^+) levels of theory. One table (S4) providing the vibrational frequencies and IR intensities for the M1[N,CO,OH]-*trans*-OH, M8[CO,OH], M1[N,CO], and M5[N,OH,OH] conformations for Li^+(Ser) calculated at the B3LYP/6-311+G(d,p) level of theory. This information is available free of charge via the Internet at http://pubs.acs.org.

References and Notes

(1) Ye, S. J.; Clark, A. A.; Armentrout, P. B. *J. Phys. Chem. B.*, submitted for publication.

(2) Dashper, S. G.; Brownfield, L.; Slakeski, N.; Zilm, P. S.; Rogers, A. H.; Reynolds, E. C. *J. Bacteriology* **2001**, *183*, 4142−4148.

(3) Moision, R. M.; Armentrout, P. B. *J. Phys. Chem. A* **2002**, *106*, 10350−10362.

(4) Moision, R. M.; Armentrout, P. B. *Phys. Chem. Chem. Phys.* **2004**, *6*, 2588−2599.

(5) Ruan, C.; Rodgers, M. T. *J. Am. Chem. Soc.* **2004**, *126*, 14600−14610.

(6) Jockusch, R. A.; Price, W. D.; Williams, E. R. *J. Phys. Chem. A* **1999**, *103*, 9266−9274.

(7) Lemoff, A. S.; Bush, M. F.; Williams, E. R. *J. Phys. Chem. A* **2005**, *109*, 1903−1910.

(8) Lemoff, A. S.; Bush, M. F.; O'Brien, J. T.; Williams, E. R. *J. Phys. Chem. A* **2006**, *110*, 8433−8442.

(9) Bush, M. F.; Forbes, M. W.; Jockusch, R. A.; Oomens, J.; Polfer, N. C.; Saykally, R. J.; Williams, E. R. *J. Phys. Chem. A* **2007**, *111*, 7753−7760.

(10) Forbes, M. W.; Bush, M. F.; Polfer, N. C.; Oomens, J.; Dunbar, R. C.; Williams, E. R.; Jockusch, R. A. *J. Phys. Chem. A* **2007**, *111*, 11759−11770.

(11) Polfer, N. C.; Oomens, J.; Dunbar, R. C. *Phys. Chem. Chem. Phys.* **2006**, *8*, 2744−2751.

(12) Kapota, C.; Lemaire, J.; Maitre, P.; Ohanessian, G. *J. Am. Chem. Soc.* **2004**, *126*, 1836−1842.

(13) Valle, J. J.; Eyler, J. R.; Oomens, J.; Moore, D. T.; van der Meer, A. F. G.; von Heldon, G.; Meijer, G.; Hendrickson, C. L.; Marshall, A. G.; Blakney, G. T. *Rev. Sci. Instrum.* **2005**, *76*, 023103.

(14) Polfer, N. C.; Oomens, J.; Moore, D. T.; von Helden, G.; Meijer, G.; Dunbar, R. C. *J. Am. Chem. Soc.* **2006**, *128*, 517−525.

(15) Polfer, N. C.; Oomens, J. *Phys. Chem. Chem. Phys.* **2007**, *9*, 3804−3817.

(16) Oepts, D.; van der Meer, A. F. G.; van Amersfoort, P. W. *Infrared Phys. Technol.* **1995**, *36*, 297−308.
(17) Pearlman, D. A.; Case, D. A.; Caldwell, J. W.; Ross, W. R.; Cheatham, T. E.; DeBolt, S.; Ferguson, D.; Seibel, G.; Kollman, P. *Comput. Phys. Commun.* **1995**, *91*, 1−41.
(18) Bylaska, E. J.; de Jong, W. A.; Kowalski, K.; Straatsma, T. P.; Valiev, M.; Wang, D.; Aprà, E.; Windus, T. L.; Hirata, S.; Hackler, M. T.; Zhao, Y.; Fan, P.-D.; Harrison, R. J.; Dupuis, M.; Smith, D. M. A.; Nieplocha, J.; Tipparaju, V.; Krishnan, M.; Auer, A. A.; Nooijen, M.; Brown, E.; Cisneros, G.; Fann, G. I.; Früchtl, H.; Garza, J.; Hirao, K.; Kendall, R.; Nichols, J. A.; Tsemekhman, K.; Wolinski, K.; Anchell, J.; Bernholdt, D.; Borowski, P.; Clark, T.; Clerc, D.; Dachsel, H.; Deegan, M.; Dyall, K.; Elwood, D.; Glendening, E.; Gutowski, M.; Hess, A.; Jaffe, J.; Johnson, B.; Ju, J.; Kobayashi, R.; Kutteh, R.; Lin, Z.; Littlefield, R.; Long, X.; Meng, B.; Nakajima, T.; Niu, S.; Pollack, L.; Rosing, M.; Sandrone, G.; Stave, M.; Taylor, H.; Thomas, G.; Lenthe, J. v.; Wong, A.; Zhang, Z. NWChem, A Computational Chemistry Package for Parallel Computers, Version 4.5, 2003, Pacific Northwest National Laboratory, Richland, Washington 99352.
(19) Roothaan, C. C. *Rev. Mod. Phys.* **1951**, *23*, 69−89.
(20) Binkley, J. S.; Pople, J. A.; Hehre, W. J. *J. Am. Chem. Soc.* **1980**, *102*, 939−947.
(21) Frisch, M. J.; Trucks, G. W.; Schlegel, H. B.; Scuseria, G. E.; Robb, M. A.; Cheeseman, J. R.; Montgomery, J. A., Jr.; Vreven, T.; Kudin, K. N.; Burant, J. C.; Millam, J. M.; Iyengar, S. S.; Tomasi, J.; Barone, V.; Mennucci, B.; Cossi, M.; Scalmani, G.; Rega, N.; Petersson, G. A.; Nakatsuji, H.; Hada, M.; Ehara, M.; Toyota, K.; Fukuda, R.; Hasegawa, J.; Ishida, M.; Nakajima, T.; Honda, Y.; Kitao, O.; Nakai, H.; Klene, M.; Li, X.; Knox, J. E.; Hratchian, H. P.; Cross, J. B.; Bakken, V.; Adamo, C.; Jaramillo, J.; Gomperts, R.; Stratmann, R. E.; Yazyev, O.; Austin, A. J.; Cammi, R.; Pomelli, C.; Ochterski, J. W.; Ayala, P. Y.; Morokuma, K.; Voth, G. A.; Salvador, P.; Dannenberg, J. J.; Zakrzewski, V. G.; Dapprich, S.; Daniels, A. D.; Strain, M. C.; Farkas, O.; Malick, D. K.; Rabuck, A. D.; Raghavachari, K.; Foresman, J. B.; Ortiz, J. V.; Cui, Q.; Baboul, A. G.; Clifford, S.; Cioslowski, J.; Stefanov, B. B.; Liu, G.; Liashenko, A.; Piskorz, P.; Komaromi, I.; Martin, R. L.; Fox, D. J.; Keith, T.; Al-Laham, M. A.; Peng, C. Y.; Nanayakkara, A.; Challacombe, M.; Gill, P. M. W.; Johnson, B.; Chen, W.; Wong, M. W.; Gonzalez, C.; Pople, J. A. *Gaussian 03*, revision D.01; Gaussian, Inc.: Pittsburgh, PA, 2005.
(22) Becke, A. D. *J. Chem. Phys.* **1993**, *98*, 5648−5652.
(23) Ditchfield, R.; Hehre, W. J.; Pople, J. A. *J. Chem. Phys.* **1971**, *54*, 724−728.
(24) McLean, A. D.; Chandler, G. S. *J. Chem. Phys.* **1980**, *72*, 5639−5648.
(25) Krishnan, R.; Binkley, J. S.; Seeger, R.; Pople, J. A. *J. Chem. Phys.* **1980**, *72*, 650−654.
(26) Foresman, J. B.; Frisch, A. E. *Exploring Chemistry with Electronic Structure Methods*, 2nd ed.; Gaussian, Inc.: Pittsburgh, PA, 1996.
(27) Hay, P. J.; Wadt, W. R. *J. Chem. Phys.* **1985**, *82*, 299−310.
(28) Glendening, E. D.; Feller, D.; Thompson, M. A. *J. Am. Chem. Soc.* **1994**, *116*, 10657−10669.
(29) Oomens, J.; Moore, D. T.; Meijer, G.; von Helden, G. *Phys. Chem. Chem. Phys.* **2004**, *6*, 710−718.
(30) Oomens, J.; Sartakov, B. G.; Meijer, G.; von Helden, G. *Int. J. Mass Spectrom.* **2006**, *254*, 1−19.
(31) Rodriguez-Santiago, L.; Sodupe, M.; Tortajada, J. *J. Phys. Chem. A* **2001**, *105*, 5340−5347.
(32) Pulkkinen, S.; Noguera, M.; Rodriguez-Santiago, L.; Sodupe, M.; Bertran, J. *Chem. Eur. J.* **2000**, *6*, 4393−4399.
(33) Jensen, F. *J. Am. Chem. Soc.* **1992**, *114*, 9533−9537.
(34) Hoyau, S.; Norrman, K.; McMahon, T. B.; Ohanessian, G. *J. Am. Chem. Soc.* **1999**, *121*, 8864−8875.
(35) Wilson, R. G.; Brewer, G. R. *Ion Beams with Applications to Ion Implantation*; Wiley: New York, 1973.
(36) Peng, C. Y.; Schlegel, H. B. *Isr. J. Chem.* **1994**, *33*, 449.
(37) Moision, R. M.; Armentrout, P. B. Manuscript in preparation.
(38) Sinclair, W. E.; Pratt, D. W. *J. Chem. Phys.* **1996**, *105*, 7942−7956.
(39) Rodgers, M. T.; Armentrout, P. B.; Oomens, J.; Steill, J. D. *J. Phys. Chem. A* **2008**, *112*, 2258−2267.
(40) Ye, S. J.; Armentrout, P. B. *J. Phys. Chem. B*, Submitted for publication.